PROPOSAL SUMMARY

PRINCIPAL INVESTIGATOR: Prof. Essam A. Marouf
Department of Electrical Engineering
San Jose State University
San Jose, CA 95192-0084
Tel. (408)924-3969
emarouf@email.sjsu.edu

PROPOSAL TITLE: Radio Occultation Investigation of the Rings of Saturn and Uranus

ABSTRACT:

a) **Objectives and Justification for Work:** The proposed work addresses two main objectives.
i) To pursue the development of the random diffraction screen model for analytical/computational characterization of the extinction and near-forward scattering by ring models that include particle crowding, uniform clustering, and clustering along preferred orientations (anisotropy). The characterization is crucial for proper interpretation of past (Voyager) and future (Cassini) ring occultation observations in terms of physical ring properties, and is needed to address outstanding puzzles in the interpretation of the Voyager radio occultation data sets.
ii) To continue the development of spectral analysis techniques to identify and characterize the power scattered by all features of Saturn's rings that can be resolved in the Voyager radio occultation observations, and to use the results to constrain the maximum particle size and its abundance. Characterization of the variability of surface mass density among the main ring features and within individual features is important for constraining the ring mass and is relevant to investigations of ring dynamics and origin.

b) **Accomplishments of Prior Year's Work:** 1) Completed the developed of the stochastic geometry (random screen) model for the interaction of electromagnetic waves with of planetary ring models; used the model to relate the oblique optical depth and the angular spectrum of the near forward scattered signal to statistical averages of the stochastic geometry of the randomly blocked area. 2) Developed analytical results based on the assumption of Poisson statistics for particle positions, and investigated the dependence of the oblique optical depth and angular spectrum on the fractional area blocked, vertical ring profile, and incidence angle when the volume fraction is small. Demonstrated agreement with the classical radiative transfer predictions for oblique incidence 3) Developed simulation procedures to generate statistical realizations of random screens corresponding to uniformly packed ring models, and used the results to characterize dependence of the extinction and near-forward scattering on ring thickness. packing fraction, and the ring opening angle.

c) **Outline of Proposed Work 1)** Extend the simulation approach to statistical realizations of random screen models that include particle crowding, clustering, and anisotropy. Characterize the dependence of the optical depth and angular spectrum on the cluster size, density, and orientation. 2) Investigate models consistent with the strength, frequency drift-rate, and bandwidth of Uranus' Ring epsilon anomalous scattered signal. Investigate potential shadowing effects on the Voyager near-grazing radio occultation geometry of the Saturn ring observations. 3) Complete the development of spectral estimation techniques to isolate and estimate the power scattered by all features of Saturn's rings that can be resolved in the measured spectrograms. 4) Use the results to estimate the maximum particle size and its abundance for each resolved feature, and to characterize the variability of the surface mass density across the ring system.

d) Marouf, E. A. , Stochastic Geometry Models for Diffraction by Planetary Rings, *BAAS* **26**, 3, 1150, 1994. Marouf, E. A., and M. K. Bird, Rosetta and Bistatic-Radar Detectability of Cometary Nuclei, Winter *AGU*, San Francisco, 1995.

I. INTRODUCTION

A three-year proposal titled "Radio Occultation Investigation of the Rings of Saturn and Uranus," was submitted to the PGG program on May 1995. It was accepted for FY 1996 funding, with progress reports due in the Spring of 1996 and the Spring of 1977. This supplement proposal is the first of the two progress reports. Section II gives a progress report on accomplishments to be completed by the end of the present funding year. Section III includes a specific statement of research proposed for the second year.

A paper reporting the nearly completed theoretical formulation of the stochastic geometry model for interaction of electromagnetic waves with spatially homogeneous planetary ring models is being prepared for submission to publication at this time.

II. PROGRESS DURING THE FIRST YEAR OF FUNDING (1/1/96-12/31/96)

Below, we discuss work completed, or in progress and is expected to be completed by the end of the present funding year.

II-A. Electromagnetic Interaction with Packed, Clustered, and Anisotropic Ring Models

A main objective outlined in the initial proposal is investigation of the problem of interaction of ring models with incident electromagnetic radiation. The ring models extend the 'classical' cloud-like many-particle-thick model to arbitrary vertical profile, and include possible packing, clustering, and anisotropy in the particle distribution.

Our approach bypasses the traditional radiative transfer based methodologies. The new approach relies on the assumption that particles of radius larger than the wavelength extinguish and diffract the incident radiation in a manner very similar to diffraction by a randomly blocked screen: the random area blocked is determined by the shadows cast by the particles on a plane normal to the direction of the incident radiation.

Our primary objectives during the present funding year is to complete the theoretical formulation of the random screen model, to compare its predictions against published results based on the traditional radiative transfer approach, and to carry out numerical simulations to extend the results to the case of uniformly packed models, for which closed-form analytical results are presently not available. Progress achieved so far and work to be completed by the end of the present funding year (by 12/31/96) are discussed briefly below.

Stochastic Geometry Model: To place the theoretical formulation of the random screen model on firm mathematical foundation, we invoke mathematical tools developed to characterize the stochastic geometry of random sets (v., e.g., Matheron, 1975, Serra, 1982, Stoyan et al., 1987, Cressie, 1993). In the rings case, the geometry of a randomly blocked diffraction screen that model the electromagnetic interaction problem (Fig. 1) is described by the a random set S composed of the union of individual particle shadow areas S_n, located at position $\mathbf{r}_n$, that is,

$$S = \bigcup_n (S_n + \mathbf{r}_n)$$

The random positions r_n form a point process in the plane of the screen. The shadow areas S_n can also be random to model random particle sizes, shape, and orientation. The union of shadow areas above define the so-called a *germ-grain* model, where r_n is a germ at which the grain S_n is placed. As outlined in the initial proposal, statistical averages of S relate to observables during a ring occultation experiment. In particular, the average area blocked p determines the extinction, hence the optical depth τ, and the covariance of S, C(r), determines the angular spectrum of the near-forward scattered signal intensity $I(\theta)$.

To obtain analytic results for p and C(r), we consider the special case when the point process r_n is Poisson distributed, that is, any position r_n can be occupied by a particle shadow with equal probability, regardless of the positions of other particles. The Poisson model allows for particle intersection when the number density is high, a physical impossibility. It applies only when the volume fraction V (the fraction of 1 m^3 of ring volume occupied by ring particles) is << 1. Note that even though the particles themselves do not intersect, their shadow areas when projected on the diffraction screen may exhibit significant overlap, depending on the observation geometry.

In the special case of a Poisson distributed r_n, the random shadow set S is called a *Boolean model* (Stoyan et al., 1987, Cressie, 1993). Its statistical averages p and C(r) may be computed from the so called 'hitting function' or 'hitting distribution,' $T_S(K)$, where

$$T_S(K) = 1 - Pr\{X \cap K = \varnothing\}$$

that is, $T_S(K)$ is the probability that the intersection of the random shadow area S with any conveniently chosen compact test set K in not empty (K hits S); $\varnothing$ is the empty set. For the Boolean model the hitting function has the analytic closed form

$$T_S(K) = 1 - exp[-\lambda E\{A(S_p)\}]$$

where E{.} denotes the expectation operator, λ is the number density of particle centers (#/m^2 of screen area), and $A(S_p)$ denotes the geometric area of the set S_p, defined as

$$S_p = \bigcup_{r \in K} S_0 + r$$

The set S_0 represents the shadow area of a 'typical' ring particle placed at the origin, and $S_0 + r$ is the same set centered at r. Appropriate choices of the test set K yield the averages p and C(r), as outlined below.

Oblique Optical Depth: As discussed in the initial proposal, the average area fraction blocked per unit screen area, p, determines the optical depth τ to be $\tau = -2 \ln(1-p)$. The area fraction p is defined as

$$p = Pr\{o \in S\} = 1 - Pr\{S \cap \{o\} = \varnothing\}$$

where {o} denotes the origin point, hence comparison with the hitting function $T_S(K)$ above indicates that p follows directly from the choice of a test set K that includes a single point, chosen for example to be the origin, that is, K={o}. Evaluation of corresponding $T_S(K)$ yields

$$\tau = \lambda E\{2\pi a^2\}$$

2

This result can be extended to oblique incidence on a slab of physical thickness d occupied by particles of number density n (particles/m^3) by realizing that when the angle between the incident wave and the ring plane is B (the ring opening angle), then the number density of the projected centers of particle shadows on the diffraction screen is given by

$$\lambda = n \, d \, / \sin(B)$$

The two equations above combine to yield exactly the same result as the classical radiative transfer result for oblique optical depth (e.g., Marouf et al., 1982). Note that $Q_{ext} = \sim 2\pi a^2$ for a particle of radius larger than a wavelength.

The $1/\sin(B)$ scaling of the oblique optical depth is, of course, valid only as long as the slab occupied by ring particles is sparsely populated (small volume fraction) so that the Poisson (Boolean) model remains valid. As discussed further below, further investigation of the scaling of τ with B for packed ring models is to be completed during the present funding year using numerical simulations.

Near-Forward Scatter: As discussed in the initial proposal, the near-forward scattered signal intensity is proportional to the angular spectrum of the random field distribution on the diffraction screen. The angular spectrum is the 2-dimensional (2-D) Fourier transform of the spatial autocovariance function $C(\mathbf{r})$, defined as

$$C(\mathbf{r}) = \Pr\{ o \notin S \text{ and } \mathbf{r} \notin S \} - (1-p)^2$$

where $\{o\}$ is the origin point and $\{\mathbf{r}\}$ is an arbitrary screen point at position vector $\mathbf{r}$. Note that

$$\Pr\{ o \notin S \text{ and } \mathbf{r} \notin S \} = \Pr\{ S \cap \{o, \mathbf{r}\} = \varnothing \}$$

The right hand side is, by definition, $1 - T_S(K)$, where the test set K in this case is the set of two points $\{o, \mathbf{r}\}$. Thus,

$$C(\mathbf{r}) = \exp[- \lambda \, E\{A(S_p)\}] - (1-p)^2$$

Analytical evaluation of the $A(S_p)$ yields exactly the same result for $C(\mathbf{r})$ as that obtained by Marouf et al. (1982) for the case of normal incidence. Extension to oblique incidence follows directly by replacing λ by $\lambda/\sin(B)$, as discussed above.

Again, validity of the analytic $C(\mathbf{r})$ above is subject to the validity of the Poisson assumption for the positions occupied by the particle centers, hence is limited to slabs of small volume fraction V. As discussed further below, numerical simulations provide an alternative approach for computing $C(\mathbf{r})$ for general packing fractions. We plan to complete a comparison between the theoretical results and the simulation results by the end of the present funding year.

Vertical Profile: We have used the stochastic geometry formulation of the extinction and near-forward scattering problems to comparatively investigate the results for two extreme vertical ring profile models, namely, a monolayer and a many-particle-thick models (referred to below as thin and thick models, respectively).

For either model, the fraction of screen area blocked p determines the optical depth to be

$\tau = -2 \ln(1-p)$. The corresponding near-forward scattered intensity $I(\theta)$ can be shown to be

$$I(\theta) = p(1-p) \, F(\theta)$$

where $F(\theta)$ is a phase-function-like parameter normalized so that its integral over the *forward* hemisphere is unity (in contrast with the traditional phase function, where the integral is taken over a 4π solid angle; $F(\theta)$ includes the contribution of near-forward diffraction only). Thus the *total* forward diffracted signal power is

$$\iint_{2\pi} I(\theta) \, d\Omega = p(1-p)$$

Note the symmetry around $p=0.5$ ($\tau = \sim 1.4$), where the peak total scattered power is achieved; a sparsely populated screen, where $p = 0.01$, for example, diffracts exactly the same total signal power as an almost fully blocked screen of $p=0.99$.

In the case of the thick model, on the one hand, $F(\theta)$ is determined by the 2-D Fourier transform of $C(r)$ above, hence is controlled by both of the particle radius a and the area fraction p. Multiple particle shadow overlaps physically correspond to multiple scattering contributions to the scattered intensity, yielding an $F(\theta)$ that may differ significantly from the single-scattering phase function. In the case of the thin model, on the other hand, $F(\theta)$ is essentially the same as the single scattering phase function, as long as the incidence direction is not near grazing (B small). At grazing incidence, the shadow areas of a particles in a crowded monolayer do overlap, hence, much like the thick model, $F(\theta)$ will differ from the single scattering phase function. Preliminary results reported below do not apply to the grazing geometry. However, the numerical simulations discussed below are expected to extend the results for the thin model to the grazing geometry.

Fig. 1 depicts the variation of the exact forward-scattered intensity $I(\theta=0)$ with oblique optical depth τ for the thin and thick models. A Henyey-Greenstein isolated particle phase function is assumed (parameter g=0.98, corresponding to an equivalent electric particle size $x=2\pi a/\lambda=\sim 100$). As expected, the models are in agreement when τ is small, but significantly differ when τ exceeds about unity. The smaller $I(0)$ for the thick case is due to the attenuation of the incident wave before it reaches the scattering particle, as well as attenuation of the scattered wave before it exits the slab.

Figs. 2-a and 2-b depict $I(\theta)$ vs. θ for the two cases $\tau=1$ and 4. Multiple-scattering within the thick model broadens the collective forward diffraction lobe and decreases its peak value. The effects become more prominent as τ increases. In the thin model case, a very large τ can only be achieved at near-grazing incidence, where significant particle shadow overlaps occur. The overlaps correspond to multiple scattering events that broaden the diffraction lobe, much like the case of the thick model. As indicated above, results depicted in Figs. 1 and 2 do not model this effect. Further work is needed to quantitatively characterize the extinction and near-forward scattering behavior of the thin model for grazing incidence. We expect to complete this characterization for the case of uniformly packed layer by the end of the present funding year.

Numerical Simulations: Analytical results reported above are valid only when that the volume fraction V of ring particles is small compared to unity. For a crowded distribution, the Poisson model for particle positions breaks down because it allows particles to intersect, which is a physical impossibility. Analytical extension of the model for V not small is difficult. As outlined

in the original proposal, the stochastic geometry model bypasses this difficulty by providing a formulation that is conveniently adaptable to numerical simulations.

For a given packing fraction V of particles of (random) radius a, occupying a slab of physical thickness d, a statistical realization of nonintersecting particles can be generated by generating first a dense uniform distribution of particle center positions. A particular position is accepted if a particle of (random) radius a placed at that position does not intersect any other previously positioned particles. The acceptance process stops when the desired volume fraction is reached.

The spatial positions of the particle centers can then be projected on a plane normal to the incidence direction and a shadow area determined by the particle radius is placed at that position. The union of all shadow areas define the geometry of a particular realization. Estimates of p and $C(r)$, computed using time-series analysis approaches outlined in the original proposal, yield estimates of the corresponding τ and $I(\theta)$. The variance of the computed estimates can be reduced by averaging the results over several simulated realizations.

The parameter space to be explored includes dependence of τ and $I(\theta)$ on the volume fraction V, physical thickness d (thin and thick rings), and ring opening angle B (incidence angle). The simulations will be conducted in collaboration with an SJSU graduate student as part of his M.S. thesis research. As initially planned, we expect to complete simulations for the case of uniformly packed models by the end of the present funding year (by 12/31/96); extension of the simulations to other interesting spatial distributions that include clustering and anisotropy is a proposed research objective for the second funding year (1/1/97-12/31/97).

III-B. Profiling Meter-Size Particles in Saturn's Rings

A second main objective outlined in the initial proposal is re-analysis of the Voyager radio occultation observations of the near-forward scattered signal in order to profile the abundance of meter-size particles in Saturn's rings with the best spatial resolution permitted by the systematic and random measurement errors. The resolution is improved by adopting a least-square modeling approach instead of a full inversion approach.

As an intermediate step towards this data processing intensive objective, we have comparatively investigated the performance of several high-resolution spectral analysis techniques optimized for tracking time-varying spectral features, similar in nature to spectral features observed. An M.S. research project by an SJSU graduate student that dealt with the comparative analysis was completed in December 1995. Selected results were summarized in the initial proposal. A search for a new graduate student to continue to collaborate on the problem is ongoing at this time. We expect that the main effort to complete tasks related to this objective will shift to the second year of funding.

5

III. PLANNED WORK FOR 1/1/97 to 12/31/97

We propose to continue investigation of problem of electromagnetic interaction with packed, clustered, and anisotropic models of planetary rings following essentially the time schedule in the initial proposal (statements 1-3 below). We also propose to continue to investigate the problem of profiling of meter size particles in Saturn's rings. The time schedule for the latter problem is adjusted to start during the second year of funding (statements 4-5 below). A statement of specific proposed research for the second funding year is given below.

1- Complete and publish results of numerical simulations for the case of uniformly packed ring models, including dependence of the oblique optical depth and the near-forward scattered intensity on ring thickness, volume fraction, and incidence angle.

2- Develop numerical simulation algorithms to generate statistical realizations of diffraction screens that simulate either uniform clustering, or clustering along preferred orientations (anisotropic distributions). The realizations should be guided by published dynamical and other physical models. Use the realizations to estimate the optical depth, correlation function, and angular spectrum, and to characterize their dependence on cluster size, density, and orientation.

3- Investigate, in the light of results obtained, models consistent with the strength, frequency drift-rate, and bandwidth of the anomalous scattered signal of Uranus' Ring epsilon. Investigate potential shadowing effects on the Voyager near-grazing radio occultation geometry of the Saturn ring observations.

4- Extend computational algorithms developed for estimation of the center frequency and drift-rate of a single spectral feature to Saturn-like multi spectral features. Estimate the center frequency and drift-rate of all features resolvable in the observed radio occultation spectrograms of Saturn's rings.

5- Design a bandpass filter bank that isolates and tracks the spectral contribution of all resolved feature. Estimate the corresponding scattered power P(t) vs. time, its peak value, and its equivalent width. Use the estimates to infer an effective particle size for each feature resolved.

REFERENCES

Cressie, N.A.C. (1993). *Statistics for Spatial Data*. John Wiley and Sons, New York.
Matheron, G. (1975). *Random Sets and Integral Geometry*. John Wiley & Sons, New York.
Marouf, E. A., Tyler, G. L., and V. R. Eshleman (1982). Theory of Radio Occultation by Saturn's Rings,"*Icarus* **49**, 161-194.
Serra, J. P. (1982). *Image Analysis and Mathematical Morphology*. Academic Press, London.
Stoyan, D., W.S. Kendall, and J. Micke (1987). *Stochastic Geometry and Its Applications*. John Wiley and Sons, New York.
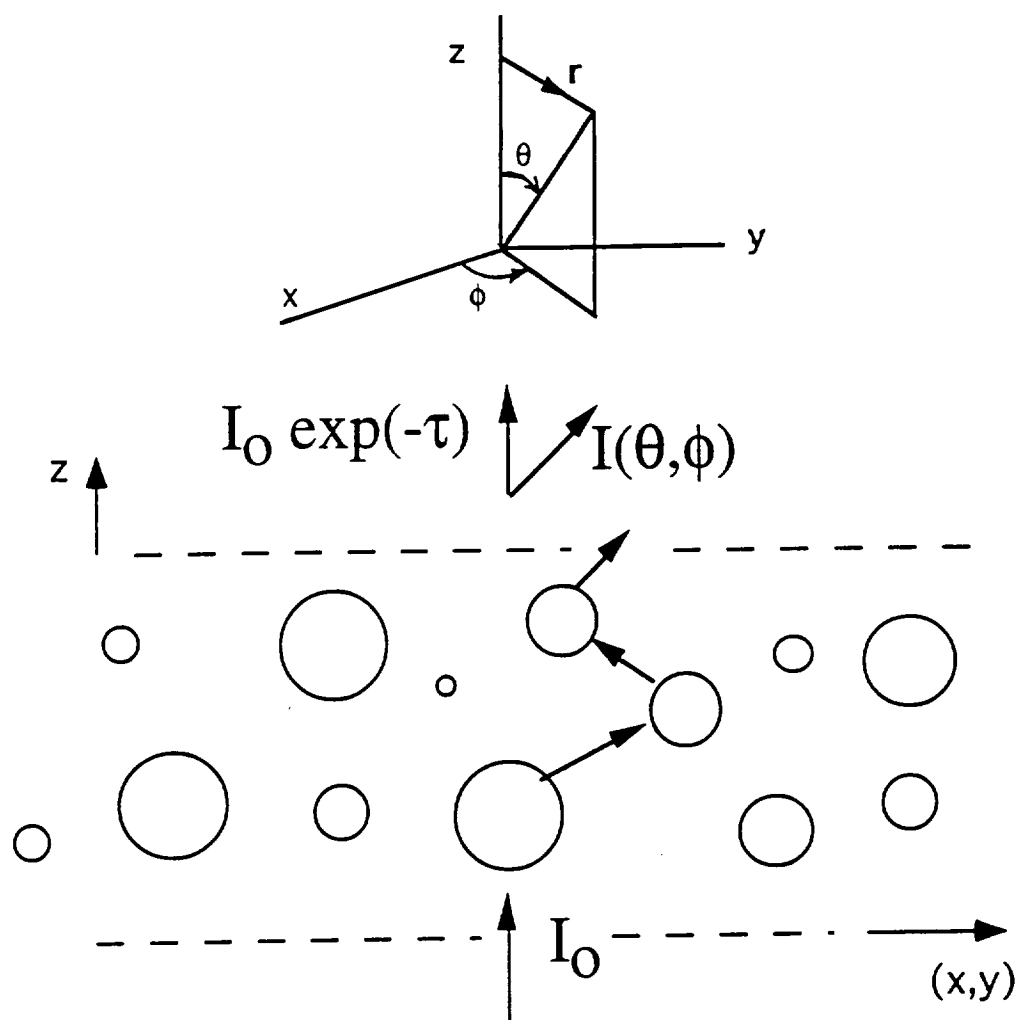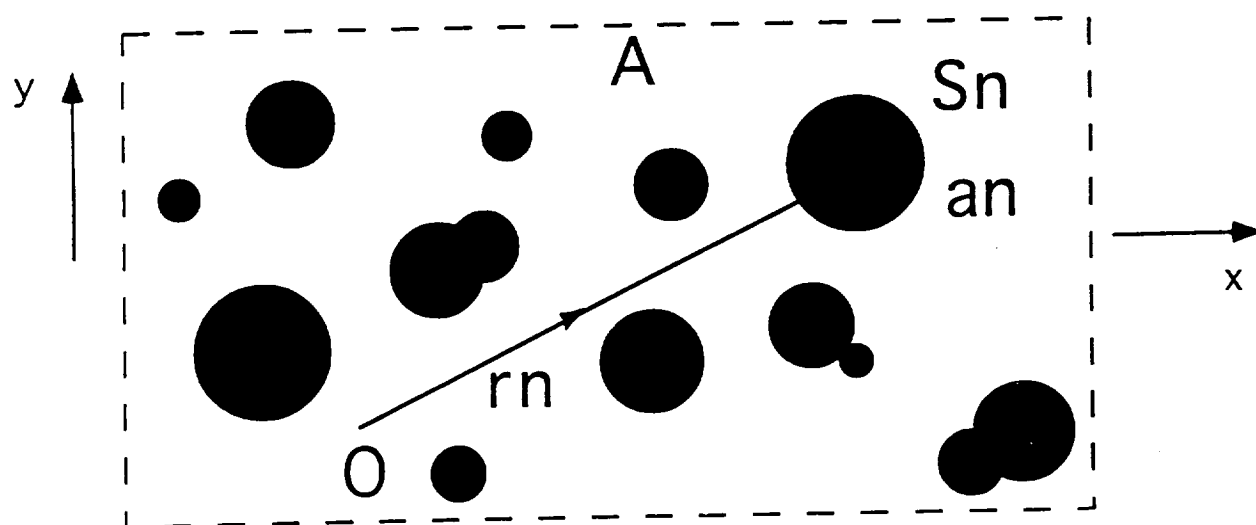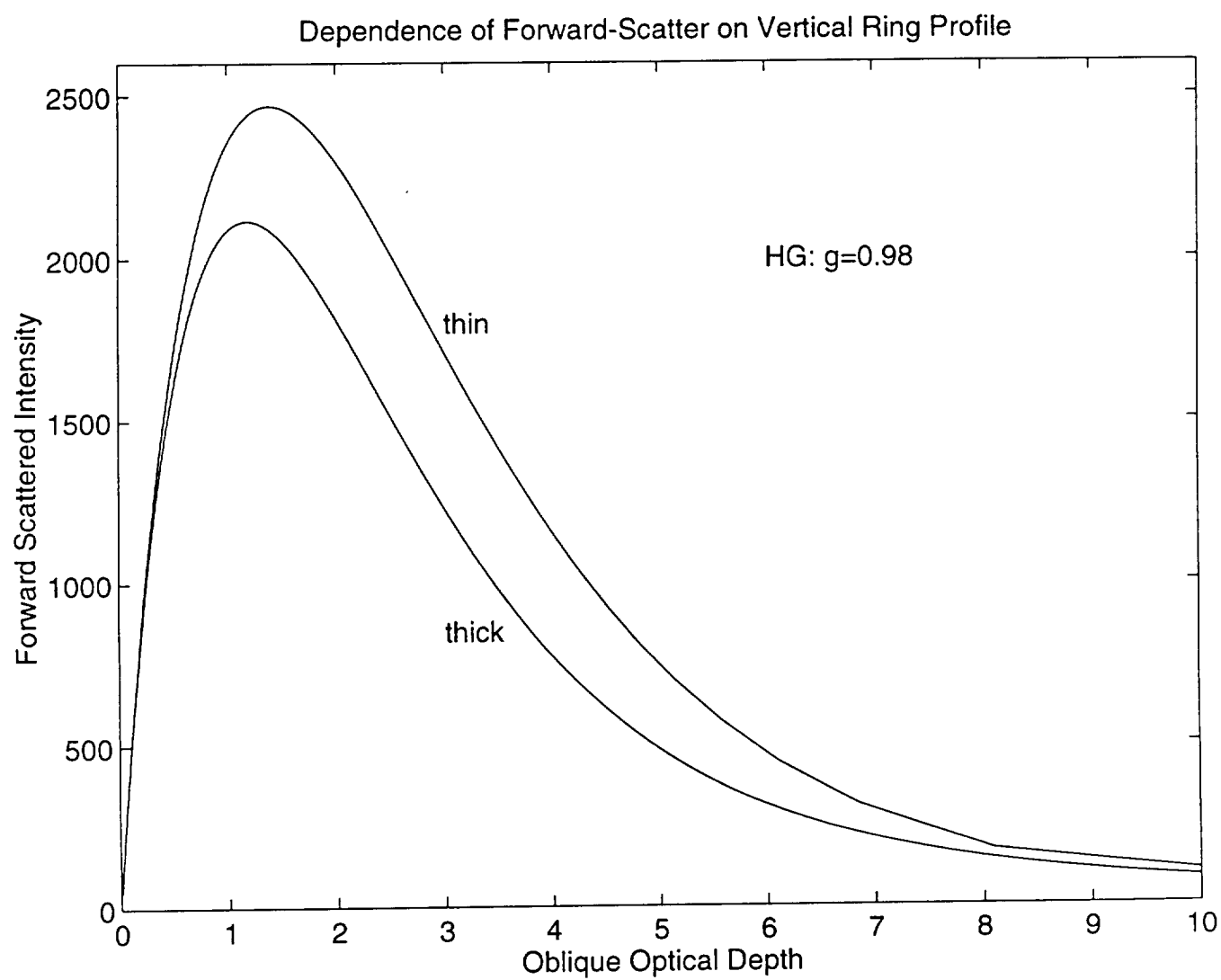
Fig. 1-a

Fig. 1-b

Fig. 2

Dependence of Forward-Scatter on Vertical Ring Profile

thin

thick

tau_q=1

HG: g=0.98

Fig. 3-a

Scattered Intensity

Normalized Scattering angle

Dependence of Forward-Scatter on Vertical Ring Profile

thin

thick

tau_q=4

HG: g=0.98

Fig. 3-b

Scattered Intensity

Normalized Scattering angle